INTERACTION NOTES

NOTE 459

October, 1984

NEW TECHNIQUES FOR THE ANALYSIS OF MULTICONDUCTOR TRANSMISSION LINES

A. H. Paxton
R. L. Gardner

Mission Research Corporation
1720 Randolph Road S.E.
Albuquerque, NM 87106

Abstract

A lumped-junction matrix method is derived for the reduction of a complicated network of branching cable bundles to an equivalent uniform section of multiconductor transmission line between two lumped junctions. The lumped junctions are represented by matrices that entirely characterize the conductors beyond the uniform section. It is shown that reflections generally favor the existence of differential propagation modes rather than common modes on conductors with significant mutual capacitance, and the degree of coupling between conductors in breakout boxes used for current and voltage measurements on shielded wires is calculated. A rate-equation approach is also derived for the calculation of the average energy flow into the various branches of a multiconductor transmission line.

CONTENTS

ILLUSTRATIONS

I. INTRODUCTION

Predicting the vulnerability of aircraft and satellites to EMP involves the analysis of the electromagnetic phenomena of geometrically complex objects. Satellites and aircraft are geometrically complex to the extent that exact analysis of the propagation of electromagnetic energy from one region of the device to other regions is impossible. This work emphasizes the coupling of electromagnetic energy into the cables and its propagation along them.

Two approaches have been applied to the problem of the propagation of pulses along the cable bundles. A computer code that uses lumped-junction techniques to obtain the signals on multiconductor transmission lines has been used to treat tubes of the cable bundles as if they were individual conductors (Ref. 1). Simplified geometries have been treated to obtain approximate peak currents. The second technique involves the use of semi-empirical set of rate equations to evaluate the average energy flow. The lumped-junction MTL model treats interference effects and calculates waveforms, but the lack of a detailed knowledge of the cable topology, as well as the simplification of the actual topology limits the extent to which the waveforms are expected to agree. It is possible to work backward and determine conditions that are possible within the available knowledge of the cable configurations, which would provide waveforms that agree qualitatively with the experiment. The rate-equation approach is an attempt to obtain approximate average agreement while either ignoring or averaging frequency-dependent interference effects.

This report is organized into five sections. Section II is a development of the lumped-junction matrix method of multiconductor transmission-line (MTL) theory. The salient assumptions and simplifications are discussed in this section. Section III is a demonstration that the physical principles that govern the propagation of electromagnetic pulses on MTLs favor the existence of differential propagation modes in the cable bundles.

---

1. Gardner, R. L., J. L. Gilbert, and L. Baker, Analytic Treatment ofCable Bundles with Large Numbers of Component Wires, AFWL-TR-83-32, Air Force Weapons Laboratory, Kirtland Air Force Base, NM February 1983.

Because reflections tend to enhance differential modes over common modes, it is unlikely that the magnitudes of the differential modes can be bounded using measurements of bulk cable currents. An estimate of the magnitude of cross-talk of wires within the breakout boxes is included in Section IV. Section V is a rate-equation formulation of the energy flow on MTLs.

II. FORMULATION OF MTL THEORY FOR APPLICATION TO THE FLTSATCOM EXPERIMENTS

First, the current in a driven, infinite MTL is obtained. The equations derived in this section, Equations 1-28, are all in the frequency domain; that is $\overline{I} = \overline{I}(\omega)$ and $\overline{V} = \overline{V}(\omega)$. The differential equations for a driven MTL are (Ref. 2, p. 98)

$$\frac{d\overline{V}}{dx} + i\omega\,\overline{\overline{L}}\,\overline{I} = \overline{G} \tag{1}$$

$$\frac{d\overline{I}}{dx} + i\omega\,\overline{\overline{C}}\,\overline{V} = \overline{D}_c \tag{2}$$

where $\overline{I}$ is the current vector, $\overline{V}$ is the voltage vector, $\overline{\overline{L}}$ and $\overline{\overline{C}}$ are the inductance and capacitance matrices, respectively, and $\overline{G}$ and $\overline{D}_c$ are the current and voltage source terms. These are combined to given an equation for the current

$$\frac{d^2\overline{I}}{dx^2} + k^2\,\overline{I} = \frac{d\overline{D}_c}{dx} - i\omega\,\overline{\overline{C}}\,\overline{G} \tag{3}$$

where

$$k = \omega/v$$

$$\frac{1}{v^2}\overline{I} = \overline{\overline{C}}\,\overline{\overline{L}}$$

This treatment assumes a single propagation velocity for the sake of simplicity, because the cable configurations are not known in enough detail to evaluate numerous propagation modes.

Assuming negligible losses in the line, the field at point x_f due to a source at point x_0 is obtained using the shift theorem for Fourier transforms (see Fig. 1). A traveling wave is shifted to an earlier time which accounts for the distance from the source by multiplying it by $\exp(-ik|x_f - x_s|)$. Therefore, the particular solution of Equation 3 that corresponds to the fields driven by the sources has the form

---

2. Frankel, Sidney, Multiconductor Transmission Line Analysis, Artech House, 1977.

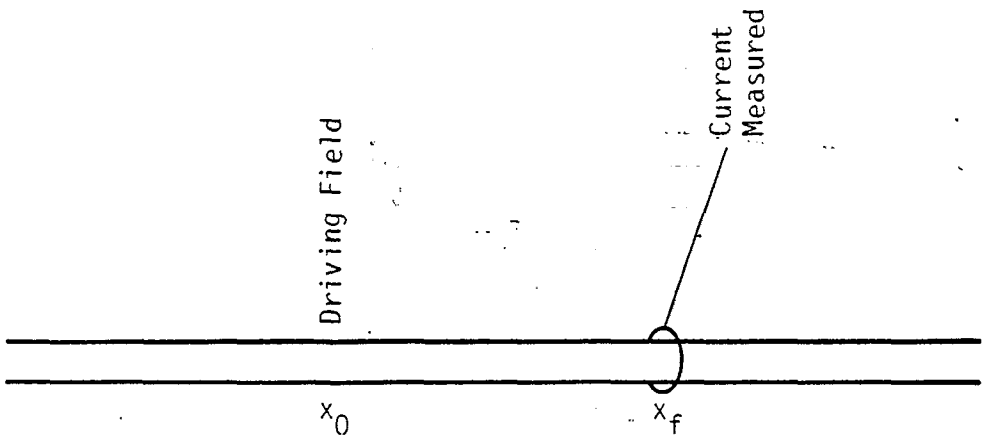

Figure 1. Infinite MTL with source point x_0 and current measurement point x_f.

$$\overline{I}(x) = \int_0^x (a\overline{G} + b\overline{D}_C) \exp(ik(x - x_0))dx_0 + \int_x^\ell (c\overline{G} + d\overline{D}_C) \exp(-ik(x - x_0))dx_0 \quad (4)$$

The substitution of Equation 4 into Equation 3 gives

$$I(x) = \frac{1}{2}\left[\int_0^x \exp(-ik(x - x_0))(\overline{D}_C(x_0) + v\overline{\overline{C}}\,\overline{G}(x_0))dx_0 + \int_x^\ell \exp(ik(x - x_0))(-\overline{D}_C(x_0) + v\overline{\overline{C}}\,\overline{G}(x_0))dx_0\right] \quad (5)$$

Equation 5 includes waves traveling in both the positive and negative directions.

If the driving fields have an extent that is small compared to the minimum wavelength of importance in the problem, Equation 5 may be rewritten

$$\bar{I}(x) = \exp(-ik(x - x_0))(\bar{I}_\ell(x_0) + \bar{I}_C(x_0))\,\theta(x - x_0)$$

$$+ \exp(ik(x - x_0))(\bar{I}_\ell(x_0) - \bar{I}_C(x_0))\,\theta(x_0 - x) \qquad (6)$$

where $\theta(y) = 1$ for $y \geq 0$ and $\theta(y) = 0$ for $y < 0$ and $\bar{I}_\ell = \int \bar{D}_L dx'$ where $\bar{D}_L = v\bar{\bar{C}}\bar{G}$ and $\bar{I}_C = \int \bar{D}_C dx'$. Equation 5 or 6 gives the current at location x of a driven MTL.

A current waveform on an MTL may be decomposed into two traveling waves. A simple junction, at which the capacitance and inductance matrices of the MTL change abruptly, may be characterized by complex frequency-independent reflection and transmission coefficients acting on the traveling wave amplitudes. Figure 2 illustrates a junction on an MTL. The current to the left of the junction is $\bar{I}_L$ and the current to the right is $\bar{I}_R$. The capacitance matrices of the two sections are $\bar{\bar{C}}_L$ and $\bar{\bar{C}}_R$. For the sake of illustration, it is assumed for now that a traveling wave moving from left to right enters the end of the MTL. A reflection matrix $\bar{\bar{R}}$ and a transmission matrix $\bar{\bar{T}}$ are defined as follows,

$$\bar{I}_R = \bar{\bar{T}}\,\bar{I}_L^+ \qquad (7)$$

$$\bar{I}_L^- = \bar{\bar{R}}\,\bar{I}_L^+ \qquad (8)$$

The reflection matrix is

$$\bar{\bar{R}} = (\bar{\bar{C}}_R - \bar{\bar{C}}_L)(\bar{\bar{C}}_R + \bar{\bar{C}}_L)^{-1} \qquad (9)$$

and the transmission matrix is

$$\bar{\bar{T}} = \bar{\bar{I}} + \bar{\bar{R}} \qquad (10)$$

A constant propagation velocity for all modes has been assumed. The convention for current used here and in the rest of this report is that positive current always moves from left to right. Of course, traveling waves that go from right to left exist, but positive current within them moves from left to right.

Having derived the reflection and transmission matrices of a single junction, it is now useful to develop the concept of the lumped junction. For the purpose of treating the propagation of electromagnetic waves along cables, it is useful to use lumped junction techniques. The junction is treated as a localized element with a complex frequency-dependent reflectivity. A length of cable with an arbitrary number of sections, each section having uniform properties, may be represented as a lumped junction. Interference effects between return waves reflected from discontinuities along the cable are treated exactly.

Consider the cable shown in Figure 2a. A pulse I^+ propagates to the right, and reflected waves return from junctions J_a and J_b, causing current I^- to propagate to the left. Although lengths L_a and L_b are different, J_b is still treated as a single junction. The entire circuit to the right of J_a may be represented by a single complex current reflection matrix, R_T for the lumped junction, Figure 2b. The reflection matrices for currents arriving from the left and right side of J_a are $\overline{\overline{R}}_{12}$ and $\overline{\overline{R}}_{21}$, respectively, as illustrated in Figure 3a. The transmission matrices are $\overline{\overline{T}}_{12}$ and $\overline{\overline{T}}_{21}$. Equations relating the current vectors to the left and right of J_a are,

$$\overline{I}_2^+ = \overline{\overline{T}}_{12}\,\overline{I}_1^+ + \overline{\overline{R}}_{21}\,\overline{I}_2^- \tag{11}$$

$$\overline{I}_1^- = \overline{\overline{R}}_{12}\,\overline{I}_1^+ + \overline{\overline{T}}_{21}\,\overline{I}_2^- \tag{12}$$

A propagation matrix, $\overline{\overline{P}}$, may be defined to propagate $\overline{I}_2^+$ and $\overline{I}_2^{-\prime}$ to obtain $\overline{I}_2^{+\prime}$ and $\overline{I}_2^-$, respectively. For the case of totally degenerate propagation modes, which is assumed in this study because the exact cable configurations cannot be treated,

$$\overline{\overline{P}}_{mn} = \delta_{mn}\exp(-ikz_n) \tag{13}$$

where z_n is the length of wire n between J_a and J_b, $k = \omega/v$, and v is the propagation velocity along the cables. The remaining equation used to obtain the lumped reflection coefficient $\overline{\overline{R}}_T$ is

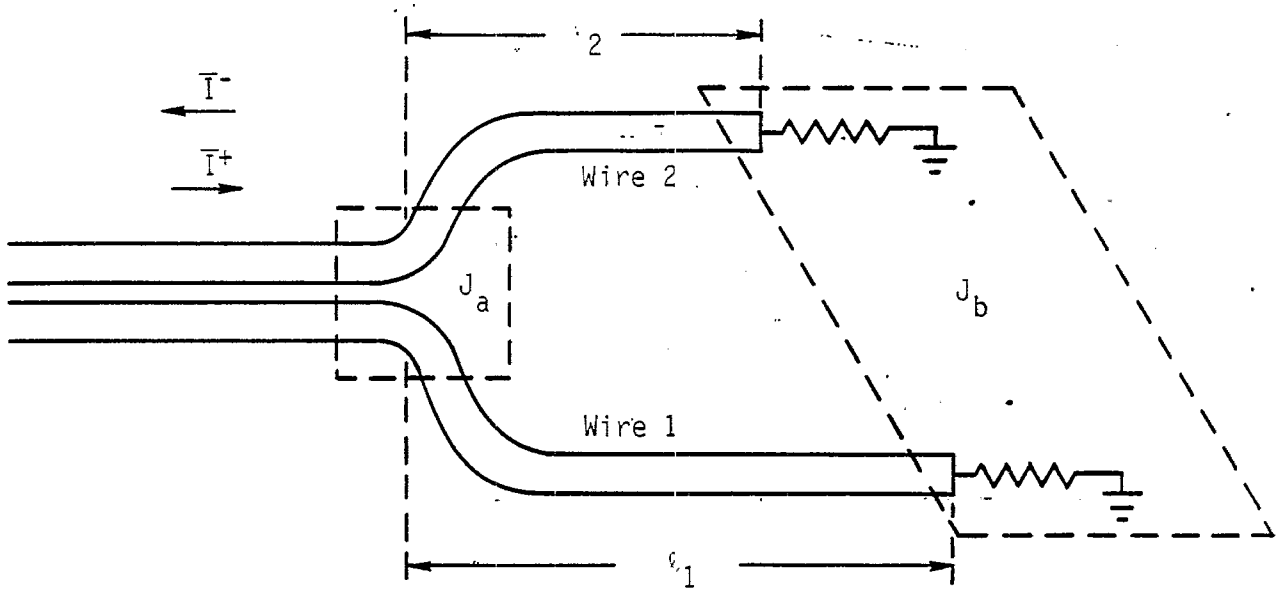

Figure 2a. Junction and terminations of wires of an MTL. J_a and J_b are the junctions.

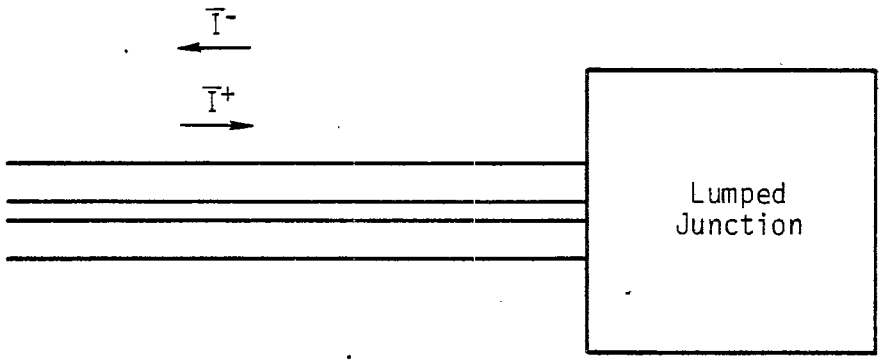

Figure 2b. Two junctions may be represented as a lumped junction.

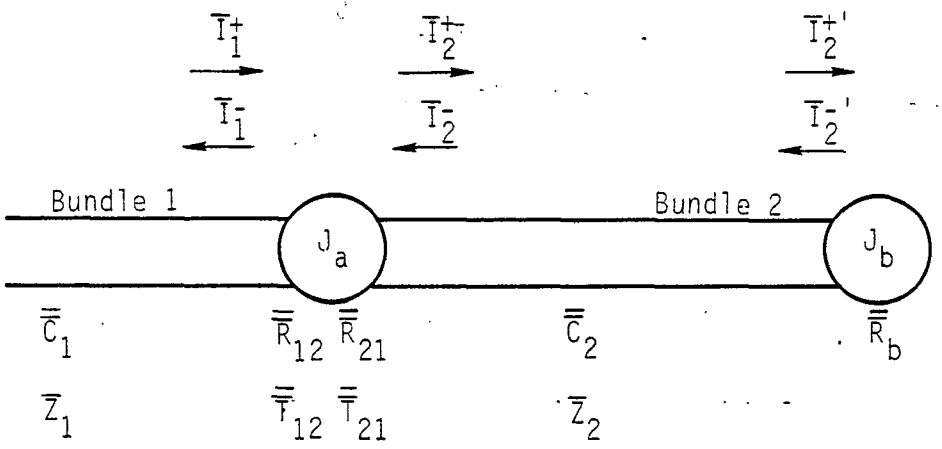

Figure 3a. Schematic of an MTL with two junctions, showing the definition of the traveling-wave currents. Positive current is always defined to be to the right, but traveling waves go in each direction.

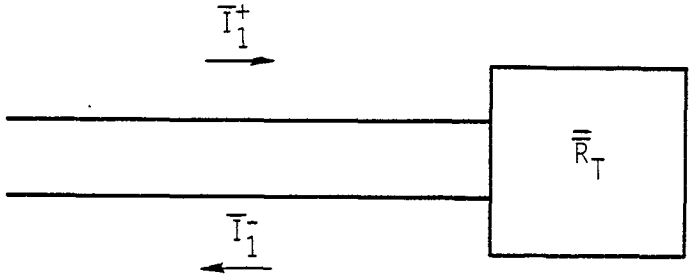

Figure 3b. The entire network to the right of Tube 1 may be characterized by a single reflection matrix, R_T.

$$\bar{I}_2^- = \bar{\bar{P}}\,\bar{\bar{R}}_b\,\bar{\bar{P}}\,\bar{I}_2^+ \tag{14}$$

The equation for $\bar{I}_1^-$ is obtained using Equations 11, 12, and 14,

$$\bar{I}_1^- = \bar{\bar{R}}_T\,\bar{I}_1^+ \tag{15}$$

where

$$\bar{\bar{R}}_T = \bar{\bar{R}}_{12} + \bar{\bar{T}}_{21}\left[\left(\bar{\bar{P}}\,\bar{\bar{R}}_b\,\bar{\bar{P}}\right)^{-1} - \bar{\bar{R}}_{21}\right]^{-1}\bar{\bar{T}}_{12} \tag{16}$$

Any number of junctions may be represented as a lumped junction by recursively applying Equation 16.

The matrix $\bar{\bar{R}}_{12}$ is obtained using Equation 9 and the other matrices of Equation 16 are related to $\bar{\bar{R}}_{12}$ as follows,

$$\bar{\bar{R}}_{21} = -\bar{\bar{R}}_{12} \tag{17}$$

$$\bar{\bar{T}}_{12} = \bar{\bar{I}} + \bar{\bar{R}}_{12} \tag{18}$$

$$\bar{\bar{T}}_{21} = \bar{\bar{I}} - \bar{\bar{R}}_{12} \tag{19}$$

Thus, a network that consists of junctions connected by sections of MTL with uniform properties may be represented by a single reflection matrix $\bar{\bar{R}}_T$ to calculate the waveform of an excited adjoining section of MTL.

The waveform on a driven section of MTL between two junctions is now obtained. An MTL with junctions at $x = 0$ and $x = \ell$ is shown in Figure 4. A current probe is located at $x = x_p$ and exciting fields act at $x = x_s$. We assume an inductively driven source current $\bar{I}_\ell$ and a capacitively driven source current $\bar{I}_C$. Because inductance-driven currents travel in the same direction just below and just above the driving point, whereas capacitance-induced currents travel in the opposite direction, the source current for the positive traveling wave is $\bar{S}^+ = \bar{I}_\ell + \bar{I}_C$ and the source current for the negative traveling wave is $\bar{S}^- = \bar{I}_\ell - \bar{I}_C$. Some interesting results of the

difference between capacitive and inductive drive for certain cable geometries are discussed in Reference 3. First equations for $\overline{I}^+(0)$ and for $\overline{I}^-(\ell)$ will be obtained in terms of R_a, R_b, S^+, and S^-, then the current at the probe location will be obtained, where R_a and R_b are the lumped reflection matrices for the networks attached to the ends of the MTL section. Equations for the current at $x = 0$ and $x = \ell$ are,

$$\overline{I}^+(0) = \overline{\overline{R}}_A \overline{I}^-(0) \tag{20}$$

$$\overline{I}^-(\ell) = \overline{\overline{R}}_B \overline{I}^+(\ell) \tag{21}$$

$$\overline{I}^+(\ell) = \overline{\overline{P}}(\ell)\overline{I}^+(0) + \overline{\overline{P}}(\ell - x_s)\overline{S}^+ \tag{22}$$

$$\overline{I}^-(0) = \overline{\overline{P}}(\ell)\overline{I}^-(\ell) + \overline{\overline{P}}(x_s)\overline{S}^- \tag{23}$$

where $\overline{\overline{P}}(d)$ is defined in Equation 13. Equations 20 through 23 are solved for $\overline{I}^+(0)$ and for $\overline{I}^-(\ell)$,

$$\overline{I}^+(0) = \left[\overline{\overline{I}} - \overline{\overline{R}}_A\overline{\overline{P}}(\ell)\overline{\overline{R}}_B\overline{\overline{P}}(\ell)\right]^{-1} \overline{\overline{R}}_A\left[\overline{\overline{P}}(\ell)\overline{\overline{R}}_B\overline{\overline{P}}(\ell - x_s)(\overline{I}_\ell + \overline{I}_C) + \overline{\overline{P}}(x_s)(\overline{I}_\ell - \overline{I}_C)\right] \tag{24}$$

$$\overline{I}^-(\ell) = \left[\overline{\overline{I}} - \overline{\overline{R}}_B\overline{\overline{P}}(\ell)\overline{\overline{R}}_A\overline{\overline{P}}(\ell)\right]^{-1} \overline{\overline{R}}_B\left[\overline{\overline{P}}(\ell)\overline{\overline{R}}_A\overline{\overline{P}}(x_s)(\overline{I}_\ell - \overline{I}_C) + \overline{\overline{P}}(\ell - x_s)(\overline{I}_\ell + \overline{I}_C)\right] \tag{25}$$

The total current at x_p is then obtained,

$$\overline{I}(x_p) = \overline{\overline{P}}(x_p)\overline{I}^+(0) + \overline{\overline{P}}(\ell - x_p)\,\overline{I}^-(\ell) + \overline{\overline{P}}(x_p - x_s)(\overline{I}_\ell + \overline{I}_C)\theta(x_p - x_s) + \overline{\overline{P}}(x_s - x_p)(\overline{I}_\ell - \overline{I}_C)\theta(x_s - x_p) \tag{26}$$

---

3. Tigner, J. E., M. J. Schmidt, P. N. Setty, and S. T. Ives, "The Excitation of Multiconductor Bundles of Wires by Electric and Magnetic Cavity Fields," IEEE Trans. on Nuc. Sci., Vol. NS-27, p. 1542, 1980.

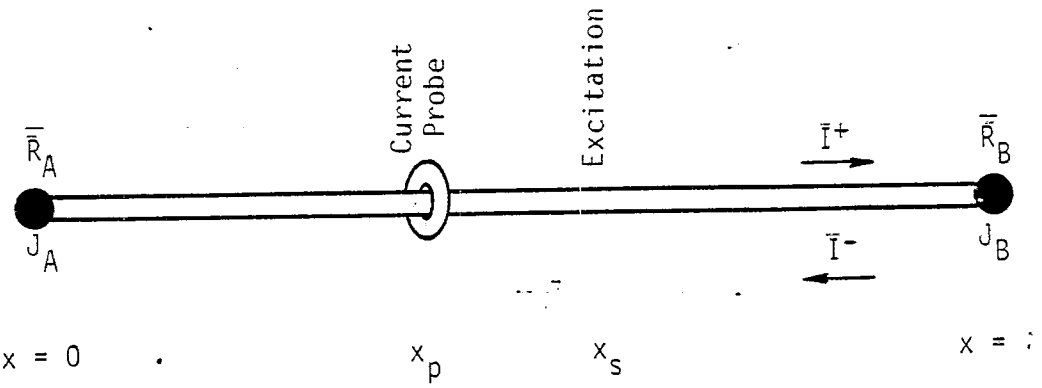

Figure 4. Section of MTL between two junctions. The excitation occurs at x_s and the current is measured at x_p.

where $\theta(y) = 1$ for $y > 0$, and $\theta(y) = 0$ for $y < 0$. Equations 24 through 26 give the current that will be measured at a probe location if the cable excitation may be treated as if it were at a point.

Equations 24 and 25 are modified to apply to extended excitation by integrating over localized source locations. For the treatment of extended excitation, the current source is represented as a current per unit length,

$$\bar{D}_L = \frac{d\bar{I}_\ell}{dx} \qquad \bar{D}_C = \frac{d\bar{I}_C}{dx} \tag{27}$$

where $\bar{D}_L = v\bar{\bar{C}}\,\bar{G}$ in Equation 5 above. The equation for the current due to the extended sources is

$$\bar{I}(x_p) = \bar{\bar{P}}(x_p)\,I^+(0) + \bar{\bar{P}}(\ell - x_p)\,\bar{I}^-(0)$$

$$+ \int_0^{x_p} \bar{\bar{P}}(x_p - x_s)(\bar{D}_L + \bar{D}_C)\,dx + \int_{x_p}^{\ell} \bar{\bar{P}}(x_s - x_p)(\bar{D}_L - \bar{D}_C)\,dx \tag{28}$$

where

$$\bar{I}^+(0) = \bar{\bar{I}} - \bar{\bar{R}}_A P(\ell)\bar{\bar{R}}_B\bar{\bar{P}}(\ell)^{-1}\,\bar{\bar{R}}_A\,\bar{\bar{P}}(\ell)\bar{\bar{R}}_B \int_0^{\ell} \bar{\bar{P}}(\ell - x_s)(\bar{D}_L(x_s) + \bar{D}_C(x_s))\,dx_s$$

$$+ \int_0^{\ell} \bar{\bar{P}}(x_s)(\bar{D}_L(x_s) - \bar{D}_C(x_s))\,dx_s$$

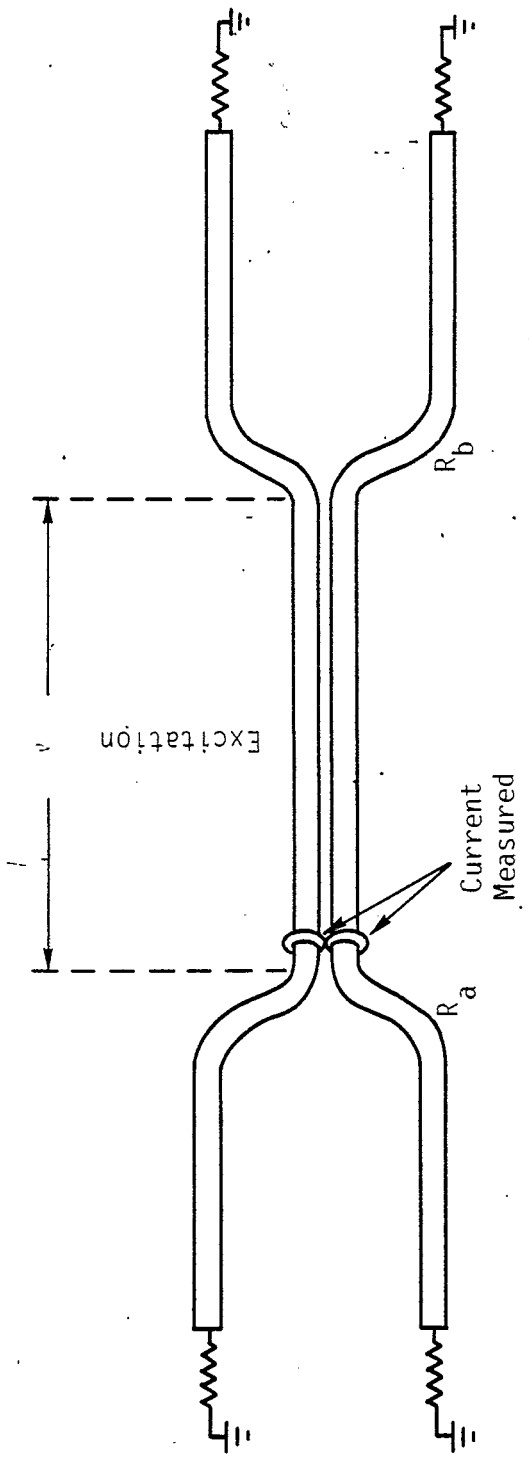

Figure 5. MTL consisting of two wires in the presence of a ground.

and

$$\bar{I}^{-}(\ell) = \left[\bar{\bar{I}} - \bar{\bar{R}}_B \bar{\bar{P}}(\ell)\bar{\bar{R}}_A \bar{\bar{P}}(\ell)\right]^{-1} \bar{\bar{R}}_B \left[\bar{\bar{P}}(\ell)\bar{\bar{R}}_A \int_0^{\ell} \bar{\bar{P}}(x_s)\left(\bar{D}_L(x_s) - \bar{D}_C(x_s)\right) dx_s + \int_0^{\ell} \bar{\bar{P}}(\ell - x_s)\left(\bar{D}_L(x_s) + \bar{D}_C(x_s)\right) dx_s\right]$$

The current vector at any location between the two lumped junctions of an MTL may be obtained using Equation 28. If the current within a section of the MTL that is represented by a lumped junction is needed, it may be obtained by exciting the end of the cable represented by the lumped junction with the waveform obtained using Equation 28.

To verify the method, a known waveform will be obtained. An MTL with two lines and a grond is illustrated in Figure 5. The resistance of the ground terminations is matched to the impedance of each cble so that no reflection occurs at any of the four wire tremination. The capacitance matrix of the middle section of MTL is

$$\bar{\bar{C}}_2 = 10^{-11}\begin{pmatrix} 3.7 & 3.8 \\ 3.8 & 2.4 \end{pmatrix} \tag{29}$$

and the capacitance matrices of the two side sections is

$$\bar{\bar{C}}_1 = \bar{\bar{C}}_3 = 10^{-11}\begin{pmatrix} 3.7 & 0 \\ 0 & 2.4 \end{pmatrix} \tag{30}$$

The reflection matrix is found using Equation 9,

$$R_a = R_b = \begin{pmatrix} 0.22 & -0.34 \\ -0.22 & 0.34 \end{pmatrix} \tag{31}$$

The reflection matrix is independent of frequency because the terminations are impedance matched. If reflections occurred at the terminations, interference effects would distort the measured pulse shape, and R would be frequency dependent. The pure differential mode, $(1,-1)/\sqrt{2}$, is an eigenvector of the reflection matrix for this case, with the diagonal elements of the capacitance matrix the same on both sides of the junction. The eigenvalue of the reflection matrix is 0.56.

The length, ℓ of the cable between the two junctions was chosen to be 12 m. A short (11 ns) differential-mode pulse shown in Figure 6 was launched by a capacitor driver at the center of the wires. The propagation time for 12 m is 40 ns, so every 40 ns a pulse that had reflected from a junction once more than the last pulse was detected at a current probe. The amplitude of each pulse was 0.56, (the calculated eigenvalue of the reflection matrix), as large as the preceding one. Thus, Figures 7 and 8 are results of calculations, using Equation 26, that are in agreement with a simple calculation. Note that the application of Equation 26 to this problem is nontrivial because the decomposition of the pulse into a frequency spectrum was followed by the operation of a matrix that contained all multiple reflections from both junctions. Then the result was transformed to obtain the time dependence.

A discussion of the influence of sections of cable bundles that loop away from the ground plane is appropriate. Such loops introduce significant inductances, which partially reflect current waves that strike them. A loop in a transmission line may be represented by inductors and a capictor inserted in the line as shown in Figure 9b. It is expected that these loops impede the flow of electrical energy between the sections of a cable bundle on the two sides of the loop if short current pulses are driven.

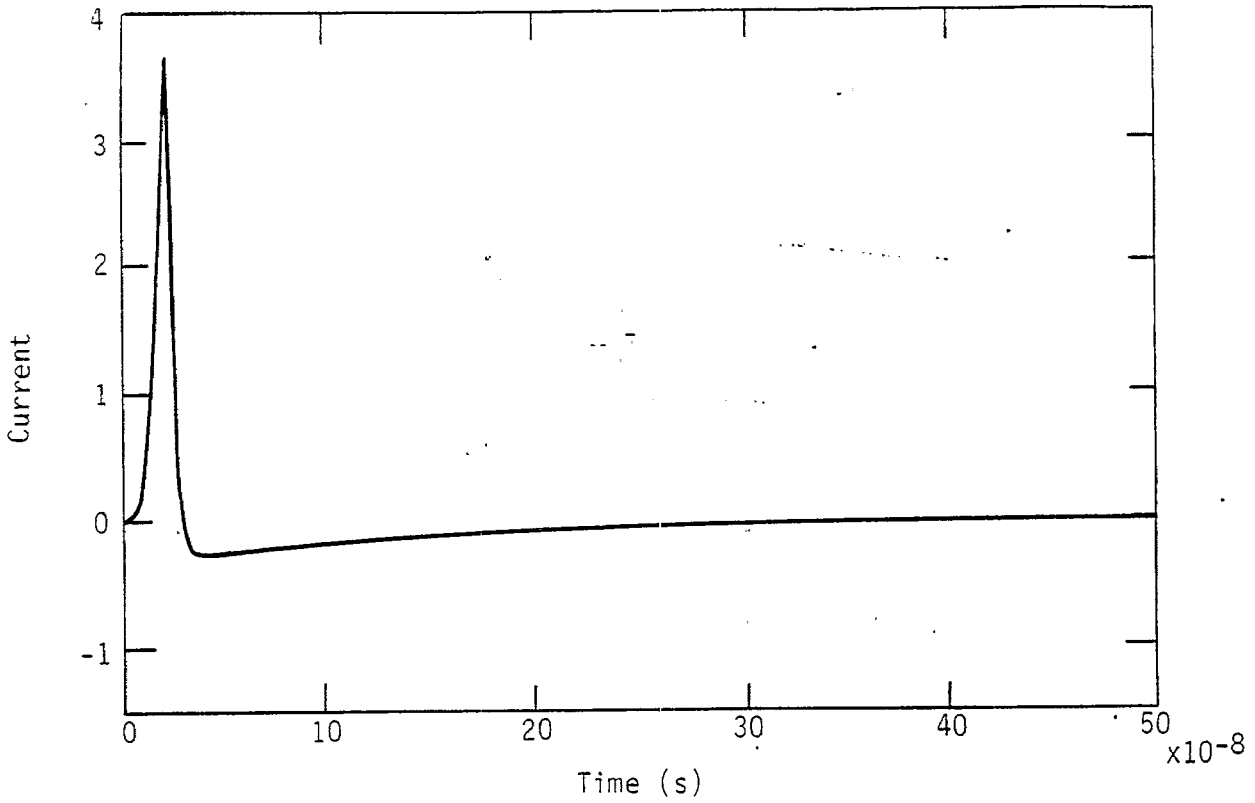

Figure 6. Differential-mode current pulse exciting the middle of the center section of the MTL shown in Figure 5.

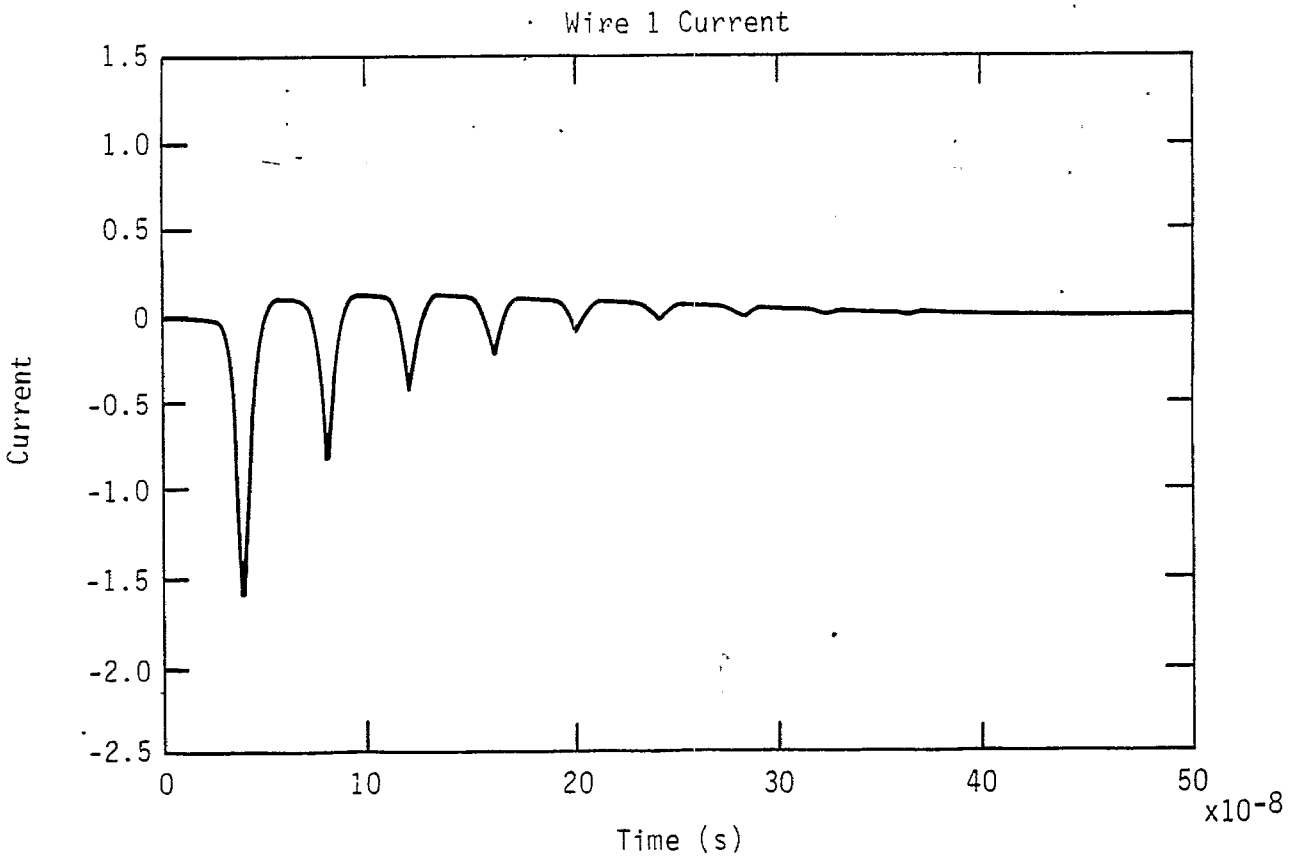

Figure 7. Current of wire 1 measured at the probe location shown in Figure 5.

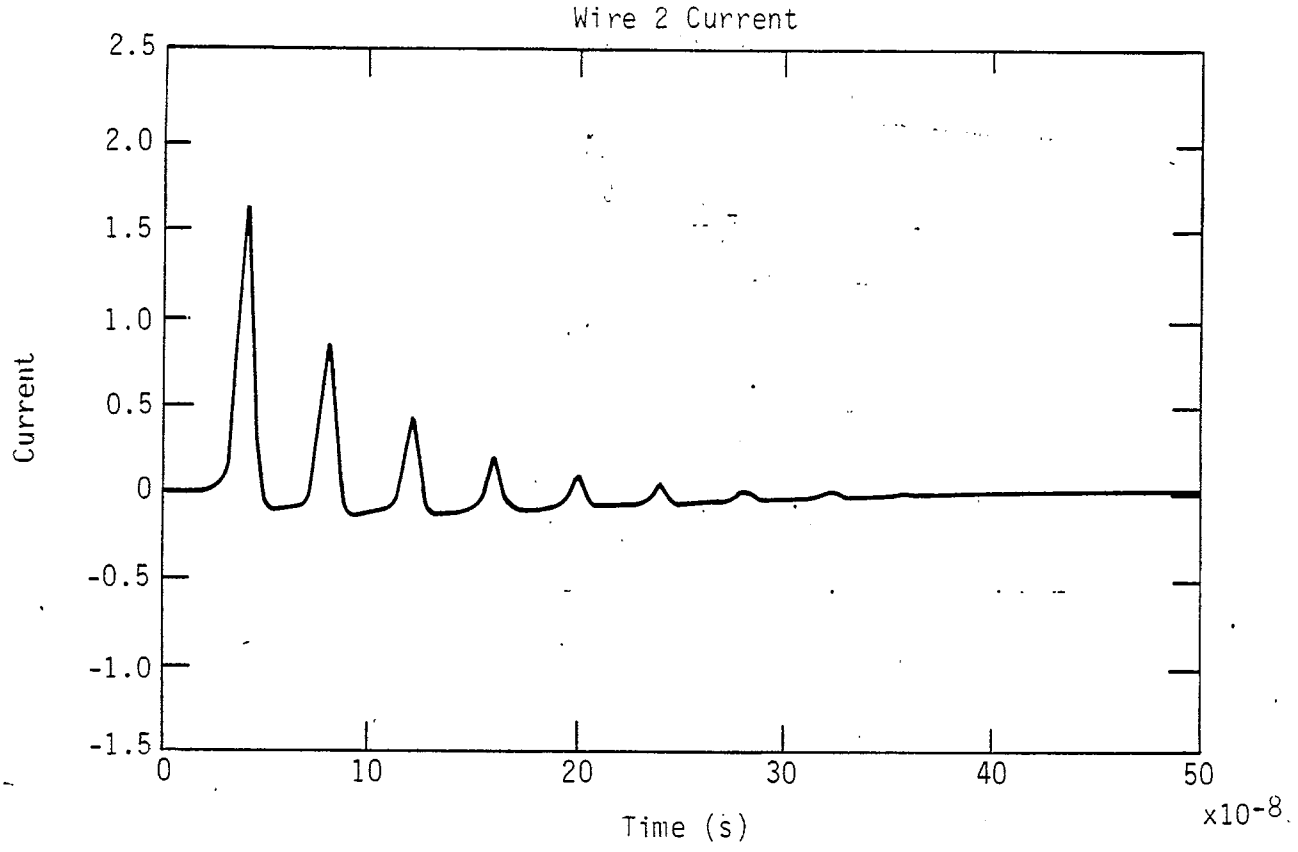

Figure 8. Current of wire 2 measured at the probe location shown in Figure 5.

The reflection factor is found to be

$$R = \frac{i\omega\left[-2L + \omega^2 L^2 C + (L_w v)^2 C\right]}{2L_w v(1 - \omega^2 LC) + 2i\omega L - i\omega^3 L^2 C + i\omega(L_w v)^2 C} \tag{32}$$

where 2L is the inductance of the loop, C is the capacitance of the wire in the loop, L_w is the inductance per unit length of the transmission line on each side of the loop, and v is the propagation velocity for waves on the transmission line. The capacitance of the wire in the loop is related to its inductance as $C \simeq x^2/Lv^2$, where $x = \pi r$ and r is the radius of the loop, which is assumed to be semicircular.

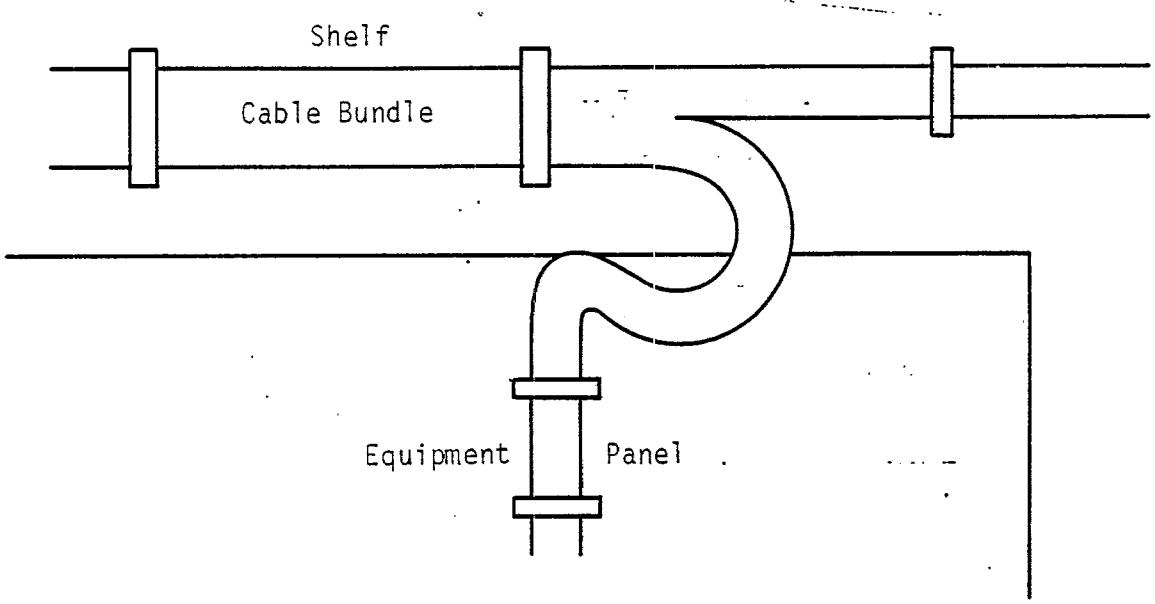

Figure 9a. Location where a section of MTL loops away from the ground plane to provide slack where it goes from the shelf to an equipment panel.

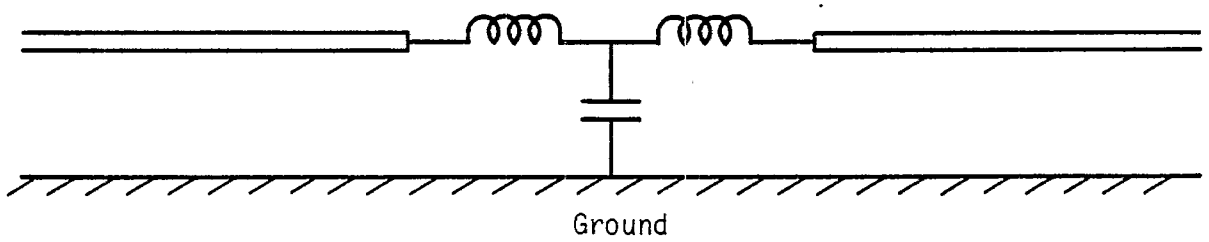

Figure 9b. Circuit equivalent to a tube that loops away from the ground plane.

The reflection coefficient is

$$R = \frac{i\omega\left[L(-2 + (kx)^2) + L_w^2 x^2/L\right]}{2L_w v(1 - (kx)^2) + i\omega L(2 - (kx)^2) + i\omega L_w^2 x^2/L} \tag{33}$$

where $k = \omega/v$ is the wave number. As an example, we consider a cable bundle attached directly to ground with an inductance per unit length of $L_w = 2 \times 10^{-7}$, and $2L = 1 \times 10^{-6}$ for the loop inductance. The average wave number for a very short pulse, intended to test the SGEMP response of a system, would be about $k = 12\ m^{-1}$, and we assume $x = 0.15$ m. For these values, to an acceptable accuracy, Equation 32 may be written,

$$R = \frac{iL((kx)^2 - 2)}{2L_w(1 - (kx)^2)/k + iL(2 - (kx)^2)} \tag{34}$$

where L is half the inductance of the loop. The magnitude of R is

$$|R| = \left[\left\{2L_w(1 - (kx)^2)/\left[Lk((kx)^2 - 2)\right]\right\}^2 + 1\right]^{-1/2} \tag{35}$$

For these values of L_w, L, and k, $|R| = 0.99$. Clearly, this process must be treated. It should be pointed out that 0.99 is not a good estimate for the average reflection coefficient, because $|R|$ decreases very rapidly with decreasing k.

III. ENHANCEMENT OF DIFFERENTIAL PROPAGATION MODES OVER COMMON MODES OF TUBES WITHIN A CABLE BUNDLE

Predicting the vulnerability of aircraft and satellites to EMP involves the analysis of the electromagnetic phenomena of geometrically complex objects. Of particular interest are bundles of cables running throughout the systems. Unfortunately, exact cable bundle configurations are not available and, moreover, it is unlikely that the cable bundles of any two devices would have the same characteristics for the propagation of pulses. In attempting to develop statistical models to bound the properties of the induced waveforms, it is useful to obtain an intuitive grasp of the connection between the bulk current and the current on individual wires or on groups of wires within a bundle. We will derive some properties of the simplest nontrivial configuration that bears on this problem, two wires in the presence of a ground conductor, as shown in Figure 10. The response of this system to an electrical excitation is obtained in terms of a two dimensional capacitance matrix.

The form of the BLT equations (Ref. 4) suggests that our conclusions may also have some validity for the analogous situation in which wire 1 and

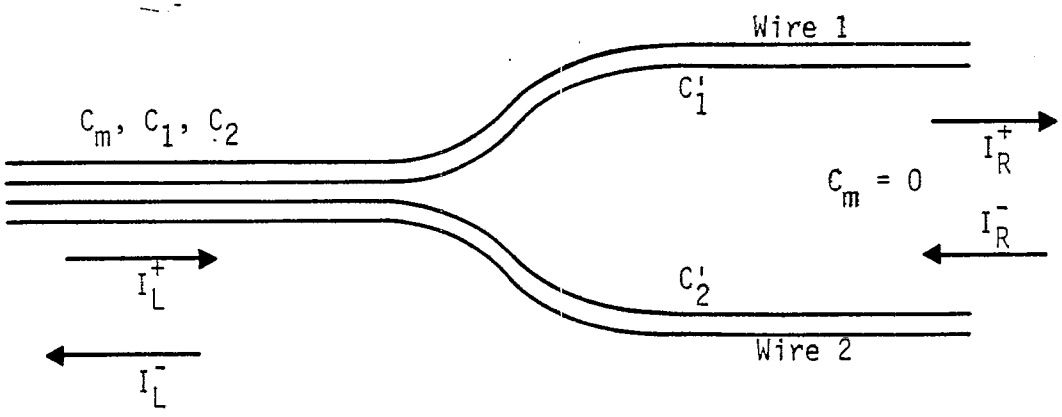

Figure 10. Infinite 2-wire transmission line with a junction.

4. Baum, C.E., T. K. Liu, and F. M. Tesche, On the General Analysis of Multiconductor Transmission-Line Networks, Interaction Notes, Note 350, Air Force Weapons Laboratory, Kirtland Air Force Base, NM, November 1978.

wire 2 are cable bundles, with capacitive coupling between the individual wires of each bundle. Then our two dimensional equations are supermatrix equations with elements that are nxn, nxm, mxn, and mxm dimensional matrices, where bundle 1 is made up of n wires and bundle 2 has m wires. The validity of the approach of treating a cable bundle as a single conducting element and a formalism for doing so has been discussed in Reference 1.

Our purpose is to illustrate that reflections at cable junctions favor differential propagation modes in the sections of the transmission line with a large mutual capacitance between the wires. One might suspect that this would be the case because a differential propagation mode with a given current is a lower energy state in a region in which the two wires under consideration are strongly capacitively coupled than in a region with weak coupling between them. The energy stored in a two-wire plus ground transmission line is

$$W = \sum_{i=1}^{2} Q_i V_i = \int dz\ \bar{V}^T \bar{\bar{C}}^T \bar{V} \tag{36}$$

where z is the coordinate along the line, $\bar{V}$ is the voltage vector, $\bar{\bar{C}}$ is the capacitance matrix, and the superscript T indicates the transpose matrix or vector. The current vector of lossless conductors in a homogeneous dielectric is related to the voltage vector by the equation,

$$\bar{I} = u\ \bar{\bar{C}}\ \bar{V} \tag{37}$$

where u is the velocity of propagation. To define the elements of the capacitance matrices, we consider a transmission line consisting of two wires and a ground as shown in Figure 10. To the left of the junction, the wires are close together and have mutual capacitance (per unit length), C_m. To the right of the junction, the mutual capacitance is zero. Capacitances to ground are C_1' and C_2' to the right of the junction, and the diagonal elements of the capacitance matrix for the section to the left of the junction are $C_1 + C_m$ and $C_2 + C_m$. The total capacitance to ground of the two wires to the left of the junction is $C_1 + C_2$. The capacitance matrices are

$$\overline{\overline{C}}_L = \begin{pmatrix} C_m + C_1 & -C_m \\ -C_m & C_m + C_2 \end{pmatrix}$$

$$\overline{\overline{C}}_R = \begin{pmatrix} C_1' & 0 \\ 0 & C_2' \end{pmatrix} \qquad (38)$$

In terms of the current vector, the energy to the left of the junction is obtained from Equation 36.

$$W = \int dz \left(\frac{1}{u^2}\right) \overline{I}^T \overline{\overline{C}}^{-1} \overline{I} = \int dz \frac{1}{u^2[C_1C_2 + C_m(C_1 + C_2)]} \left[I_1^2C_2 + I_2^2C_1 + 2I_1I_2C_m\right] \qquad (39)$$

The energy is clearly lower if $I_2 = -I_1$, than if $I_2 = I_1$, for the same value of I_1, which demonstrates that the differential mode is a lower energy state than the common mode in a section of line with nonzero mutual capacitance, C_m.

For a mode with the same currents, the energy to the right of the junction is

$$W' = \int dz \frac{1}{u^2C_1'C_2'} \left[I_1^2C_2' + I_2^2C_1'\right] \qquad (40)$$

Conditions that will frequently be satisfied are: $C_m > C_1'$, $C_m > C_2'$, C_1 similar in magnitude to C_1', C_2 similar in magnitude to C_2'. For configurations that satisfy these conditions, W will clearly be significantly lower than W' for the differential mode, $I_2 = -I_1$. This demonstrates that the differential mode has a lower energy in a section of transmission line with strong mutual capacitive coupling than in a section of line with no mutual capacitance, unless the capacitance to ground is much larger in the latter section.

A general set of equations, known as the BLT equations (Ref. 4) is used for the analysis of multiconductor transmission lines. To solve for the currents to the left and to the right of the junction, the BLT equations have solutions that may be written in terms of reflection and transmission matrices.

We define reflection and transmission matrices, R_R, R_L, T_R, T_L,

$$\bar{I}_L^- = \bar{\bar{R}}_L \bar{I}_L^+ + \bar{\bar{T}}_R \bar{I}_R^-$$

$$\bar{I}_R^+ = \bar{\bar{T}}_L \bar{I}_L^+ + \bar{\bar{R}}_R \bar{I}_R^-$$

Conservation of charge and the continuity of voltage along a wire, together with equations relating current to voltage in a multiconductor transmission line may be used to obtain equations for the reflection and transmission matrices,

$$\begin{aligned}
\bar{\bar{R}}_L &= (\bar{\bar{C}}_R - \bar{\bar{C}}_L)(\bar{\bar{C}}_L + \bar{\bar{C}}_R)^{-1} \\
\bar{\bar{R}}_R &= -\bar{\bar{R}}_L \\
\bar{\bar{T}}_L &= \bar{\bar{I}} + \bar{\bar{R}}_L \\
\bar{\bar{T}}_R &= \bar{\bar{I}} - \bar{\bar{R}}_L \quad ,
\end{aligned} \tag{41}$$

where $\bar{\bar{I}}$ is the identity matrix.

The elements of $\bar{\bar{R}}_L$ are

$$\begin{aligned}
R_{L11} &= -\frac{1}{D}\left[C_m(C_1 - C_1' + C_2 + C_2') + (C_1 - C_1')(C_2 + C_2')\right] \\
R_{L22} &= -\frac{1}{D}\left[C_m(C_1 + C_1' + C_2 - C_2') + (C_1 + C_1')(C_2 - C_2')\right] \\
R_{L12} &= \frac{1}{D} 2C_m C_1' \\
R_{L21} &= \frac{1}{D} 2C_m C_2'
\end{aligned} \tag{42}$$

where

$$D = (C_m + C_1 + C_1')(C_m + C_2 + C_2') - C_m^2$$

The off-diagonal elements are always positive. Both diagonal elements will frequently be negative. In the example we discuss below, R_L has negative diagonal elements, and the properties we derive result from this feature.

The reflection and transmission matrices depend on the relative values of the capacitances, but all capacitances may be multiplied by the same number without affecting them. We use the following capacitance values to illustrate the properties of the reflection and transmission matrices at a junction.

$$C_1 = 0.4\ C_m\ , \quad C_1' = 0.6\ C_m\ , \quad C_2 = 0.6\ C_m\ , \quad C_2' = 0.8\ C_m\ .$$

These capacitances correspond to conductors that are quite close to the ground plane. Using these values, we obtain

$$R_L = \begin{pmatrix} -0.242 & 0.316 \\ 0.421 & -0.158 \end{pmatrix} .$$

The eigenvalues and eigenvectors of this matrix are

$$\lambda_1 = -0.567 \qquad I_1 = \begin{pmatrix} 0.70 \\ -0.72 \end{pmatrix}$$

$$\lambda_2 = 0.167 \qquad I_2 = \begin{pmatrix} 0.61 \\ 0.79 \end{pmatrix} .$$

The physical interpretation of these eigenvalues is that they are the amplitude reflectivities of the current eigenvectors incident on the junction from the left. The eigenvectors are not orthogonal. The matrices R_R, T_R, and T_L have the same eigenvectors as R_L, but their eigenvalues are different.

The eigenvector I_1, which has almost no bulk current, will tend to remain to the left of the junction, since it has reflection coefficient 0.567, while I_2 is mostly transmitted. One might expect this to be the case, because I_1 is a lower energy state for a given current magnitude to the left of the junction, while I_2 is not. A differential mode will tend to remain in the part of a circuit with an appreciable mutual capacitance. A common propagation mode does not strongly favor either side of the junction for the case $C_1 + C_2 \approx C_1' + C_2'$.

The transmission matrix is $\overline{\overline{T}}_L = \overline{\overline{I}} + \overline{\overline{R}}_L$, where $\overline{\overline{I}}$ is the unit matrix. The eigenvalues of $\overline{\overline{T}}_L$ that correspond to $\overline{I}_1$ and $\overline{I}_2$ are

$$\lambda_1^T = 1 + \lambda_1 = 0.433$$

$$\lambda_2^T = 1 + \lambda_2 = 1.167 \quad ,$$

so a common mode has a much larger coefficient for transmission out of the region where the wires are close together, than a differential mode.

It can be shown that in the limit $C_m \gg C_1, C_2, C_1', C_2'$ the pure differential mode is an eigenvector of R_L with eigenvalue 1; the differential mode becomes totally trapped in the left section of the line. Our numerical example above is not very extreme considering this possibility. The mutual capacitance between two sections of a cable that split into individual cables would usually be larger with respect to C_1, C_2, C_1', and C_2' than in the numerical example. For this case λ_1 would be larger and so would $\lambda_1^{T'}$, leading to further enhancement of the differential mode in the segment with an appreciable mutual capacitance.

It is also interesting to consider a current vector approaching the junction from the right. For the case of a pulse, only in one wire, incident on the junction from the right, the current passing through to the left of the junction will consist primarily of a differential propagation mode. The eigenvalues corresponding to the transmission coefficients of current vectors incident on the junction from the right are

$$\lambda_1^{T'} = 1.567 \quad , \quad \text{corresponding to} \quad I_1 = \begin{pmatrix} 0.70 \\ -0.72 \end{pmatrix}$$

and

$$\lambda_2^{T'} = 0.833 \quad , \quad \text{corresponding to} \quad I_2 = \begin{pmatrix} 0.61 \\ 0.79 \end{pmatrix}$$

Suppose that a current pulse arrives at the junction only in wire 1.

$$I = \begin{pmatrix} 1 \\ 0 \end{pmatrix}$$

In terms of the eigenvectors,

$$I_T = aI_1 + bI_2$$

$$a = 0.79 \qquad b = 0.72 \ .$$

The incident current is about equally divided between the two eigenvectors. Multiplying the coefficients of the eigenvectors by the eigenvalues, the transmitted current vector is obtained,

$$I_T = \begin{pmatrix} 1.23 \\ -0.42 \end{pmatrix}$$

The current in wire 1 is much larger than the bulk current in the circuit, to the left of the junction. That is, the charge in wire 1 induces a charge in wire 2 with the opposite sign, due to the mutual capacitance. This is an example of a situation in which a current in a portion of an MTL is much larger than the bulk current in the MTL.

While this example does not address all the complicated interference effects that take place in airplane and satellite circuits, it does indicate that the measurement of bulk currents of cable bundles will not provide estimates of individual wire currents in a simple manner because reflections at the cable junctions favor the existence of differential propagation modes.

IV. BREAKOUT BOX CROSSTALK

Breakout boxes are sometimes used in testing devices for EMP hardness. Cables shields terminate at the entry to the breakout box and the insulated wires inside the coaxial cable shield continue on into the breakout box to the interior box connector as shown in Figure 11. The worst case for potential crosstalk corresponds to a pair of wires so close together that their insulation touches over a distance of some 5 cm. That close configuration was chosen for the example analysis which follows.

The analysis was carried out using the methods developed in Reference 1 and are used regularly throughout the rest of this report in which the cables or groups of cables are treated as tubes and the various discontinuities in the cable bundle geometry are treated as junctions. This methodology is consistent with the formulation of the BLT equation (Ref. 4). The specific geometry is shown in Figure 11. Incident currents I^i in the coaxial cables are shown on the left. Since the currents propagate within the coaxial cable the exact path the cable follows as it enters the breakout box is immaterial to the analysis. As the cable enters the breakout box the cable geometry is treated as a junction with complex terminations to include the change in self inductance and capacitance as well as mutual terms to account for the cross coupling. The values of the various impedance elements are calculated entirely from geometric considerations with the following results.

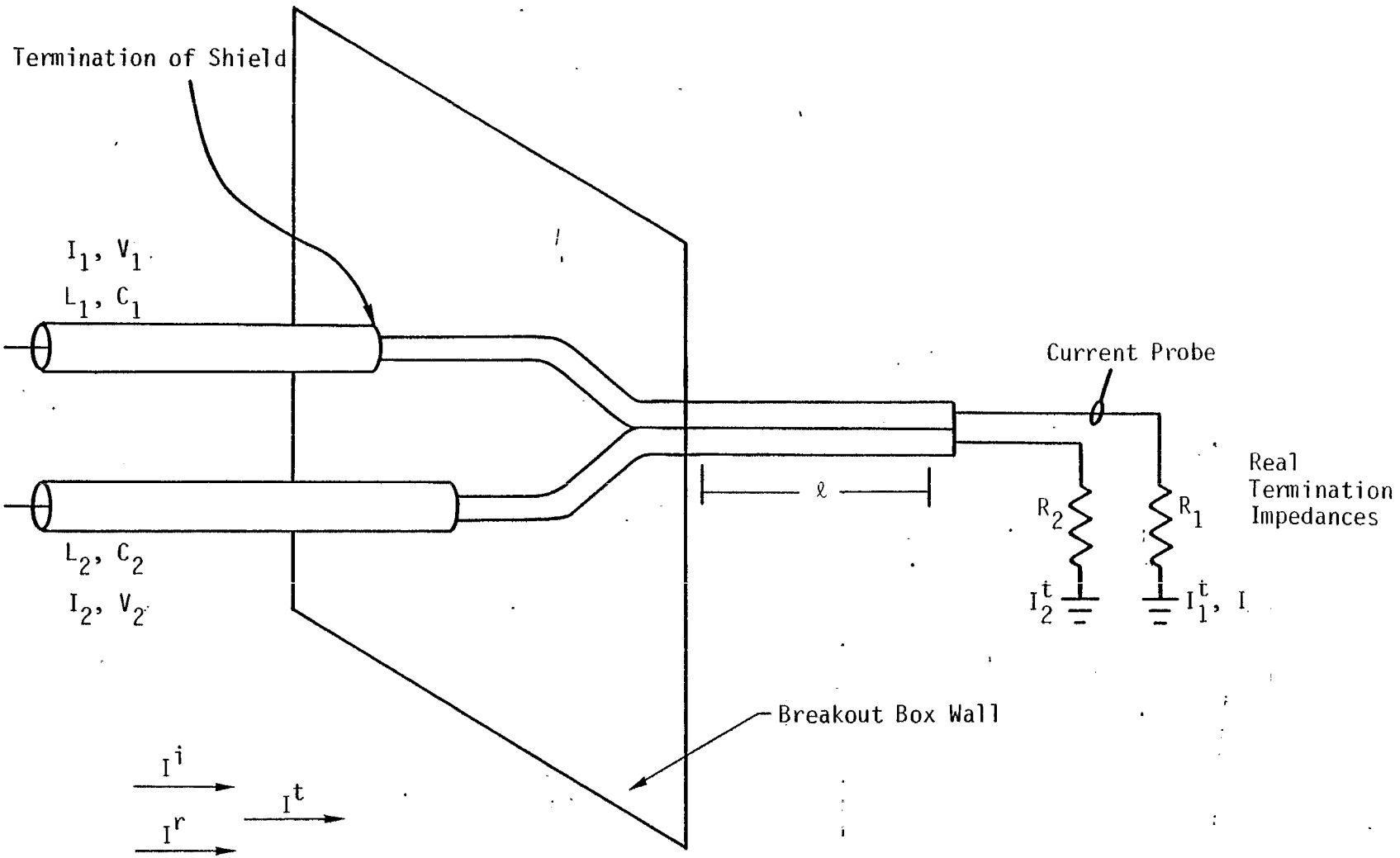

Figure 11. Two 1S20 cables entering breakout box with section ℓ meters long section of two insulated wires as close as possible to each other.

The inductance and capacitance per unit length, impedance, and the propagation velocity of 1S20 cables, selected as an example are,

$$L_w = 9.6 \times 10^{-8} \text{ Hz/m}$$

$$C_w = 8.0 \times 10^{-10} \text{ F/m}$$

$$v = 1.14 \times 10^{8} \text{ m/s}$$

$$Z_w = 11 \ \Omega$$

Within the box, shields on the cables have been removed leaving only insulated wires over a ground plane. Mutual coupling between the wires is calculated by assuming the wires have their insulations touching over a 5 cm length and the wires are 5 cm from a ground plane. Effects of the other 5 sides of the box were ignored. The self and mutual capacitances of the wires found were

$$C_s = 5.97 \times 10^{-12} \text{ F/m}$$

$$C_m = 9.67 \times 10^{-11} \text{ F/m}$$

The capacitance matrix of the interior of the breakout box is then

$$C_2 = \begin{bmatrix} C_s + C_m & -C_m \\ -C_m & C_s + C_m \end{bmatrix} \tag{43}$$

The elastance matrix P_2 is

$$P_2 = C_2^{-1} \tag{44}$$

and the load impedance matrix for the terminations is

$$Z_L = R_L + \frac{j\omega\ell}{v^2} P_2$$

$$= \begin{bmatrix} R_1 & 0 \\ 0 & R_2 \end{bmatrix} + \frac{j\omega\ell}{v^2} \begin{bmatrix} C_s & -C_m \\ -C_m & C_s \end{bmatrix}^{-1} \tag{45}$$

The admittance matrices for the incident cables (subscript 1 in Fig. 11) and the termination sections (subscript 2 in Fig. 11) are then

$$Y_1 = v\, C_1 = v \begin{bmatrix} C_w & 0 \\ 0 & C_w \end{bmatrix} \tag{46}$$

$$Y_2 = Z_L^{-1} \tag{47}$$

Finally, the current transmitted into the junction is given by Reference 1

$$I^t = 2Y_2(Y_1 + Y_2)^{-1}\, Y_1 V^i \tag{48}$$

In order to estimate crosstalk only cable 1 was driven so that

$$V^i = \begin{pmatrix} 1 \\ 0 \end{pmatrix} \tag{49}$$

The measure of crosstalk chosen was I_2^t/I_1^t. Current I_2^t is that current which results when a current enters on cable 1 (I_1^i) and is reflected back out cable 2 (I_2^r). (From Kirchoff's laws $I_2^t = I_2^r$.) Note that this ratio has no limit since an extreme case (if non-physical) is all of the current entering I_1^i could be reflected back as I_2^r.

An investigation of more realistic cases, however, revealed that crosstalk can be a problem at high frequencies. The results of two sample cases is

shown in Figure 12. The first case is for $R_1 = R_2 = 100\ \Omega$. This case resulted in wire 2 carrying a maximum of 0.3 of the wire 1 current at 150 MHz. At higher frequencies, the fraction may be larger, of course. The model used here is not valid for frequencies above a few hundred MHz, however. As a more pathological case, R_1 was chosen as 100 Ω and wire 2 resistance was chosen as 10 Ω. At high frequencies the two wires carried essentially equal currents. It is clear from these calculations that breakout box crosstalk can be a problem under certain conditions.

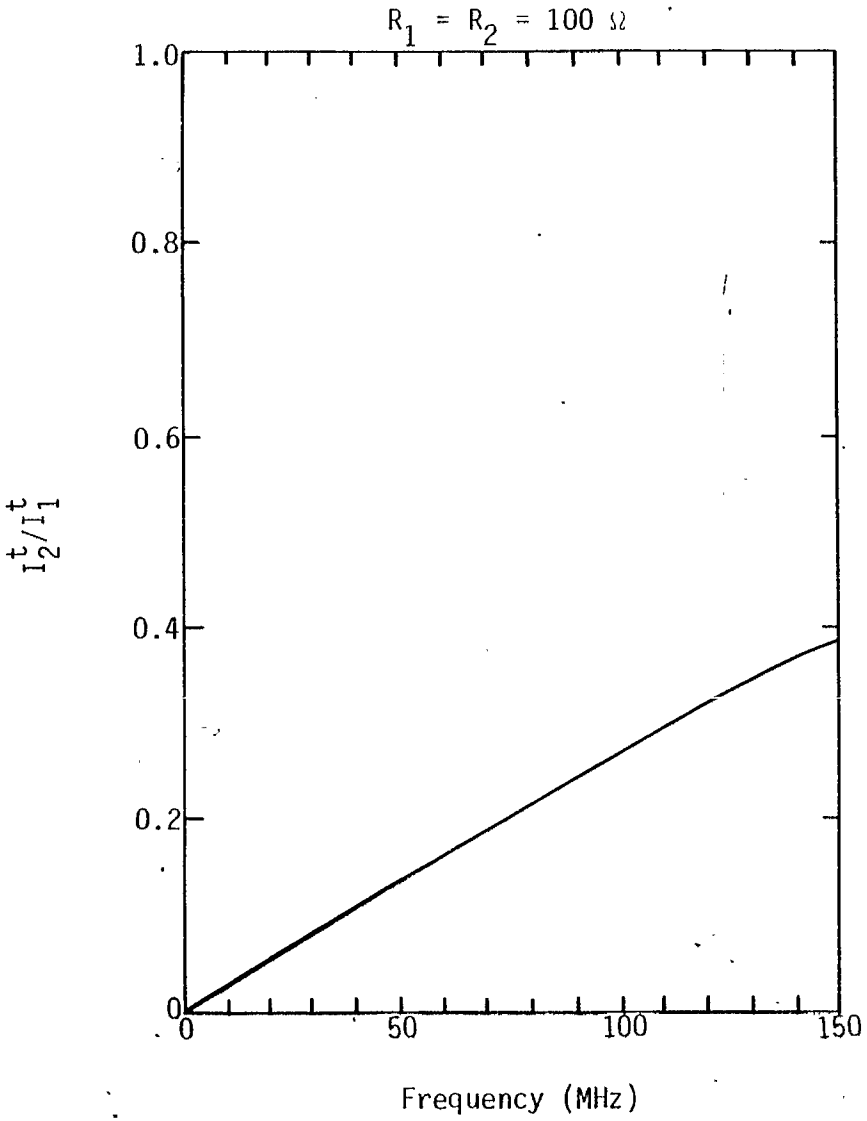

Figure 12a.

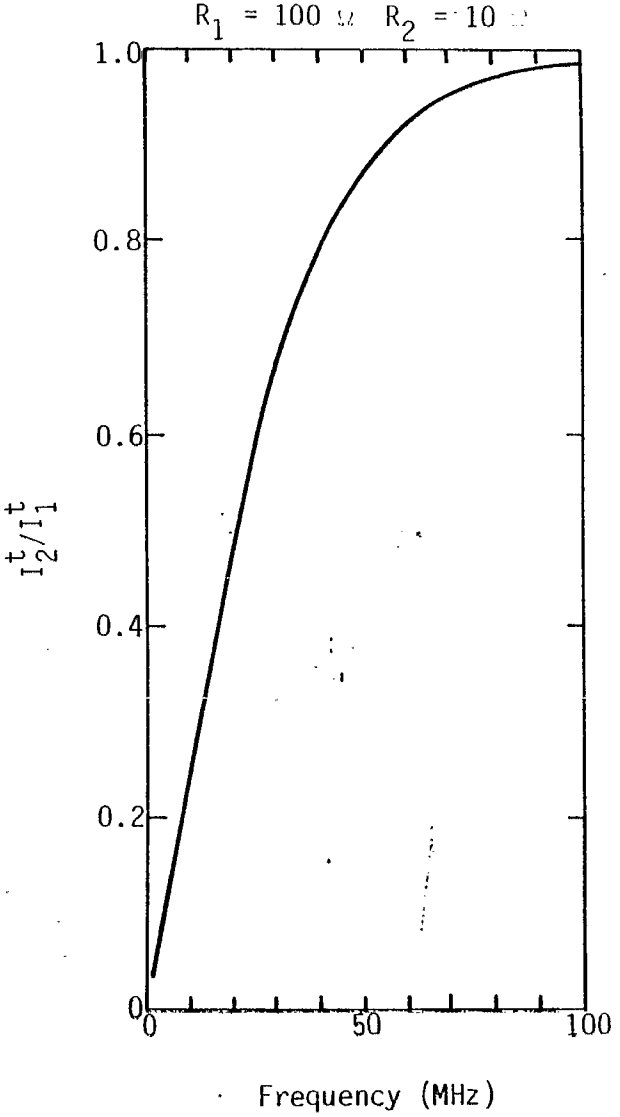

Figure 12b.

Figure 12. Plots of I_2^t/I_1^t as a function of frequency, indicating the degree of crosstalk for the breakout box geometry shown in Figure 11.

V. RATE-EQUATION TREATMENT OF ENERGY FLOW

An approximate rate-equation treatment for the energy flow along a MTL may provide the most accurate means of estimating currents on the shields of cable bundles that are too complicated or not well enough characterized for an exact treatment. Interference effects are ignored so that exact waveforms cannot be obtained nor can resonant effects that are highly wavelength selective be treated. It is important to note, however, that these effects cannot be treated by other means unless the precise cable geometry is known and modeled.

The energy per unit length stored in a traveling wave on a multiconductor transmission line is

$$W = \frac{1}{v} \bar{I}^T \bar{V} \tag{50}$$

and the energy flow is

$$S = \bar{I}^T \bar{V} \tag{51}$$

Therefore, for a single-mode MTL, the energy is

$$W = \bar{I}^T \bar{\bar{L}} \bar{I} \tag{52}$$

The energy transmission factor for transfer from length L to length R, F_{LR}, is defined by the equation

$$S_{LR} = F_{LR} v W_L / 2 \tag{53}$$

where S_{LR} is the rate of energy flow through the junction and W_L is the energy per unit length in both traveling waves on the left length of the MTL.

In terms of the right-traveling wave,

$$S_{LR} = \frac{1}{v} \bar{I}_R^{+T} \bar{\bar{C}}_R^{-1} \bar{I}_R^{+} \tag{54}$$

The currents $\bar{I}_R^+$ and $\bar{I}_L^+$ are related by the transmission matrix $\bar{\bar{T}}$,

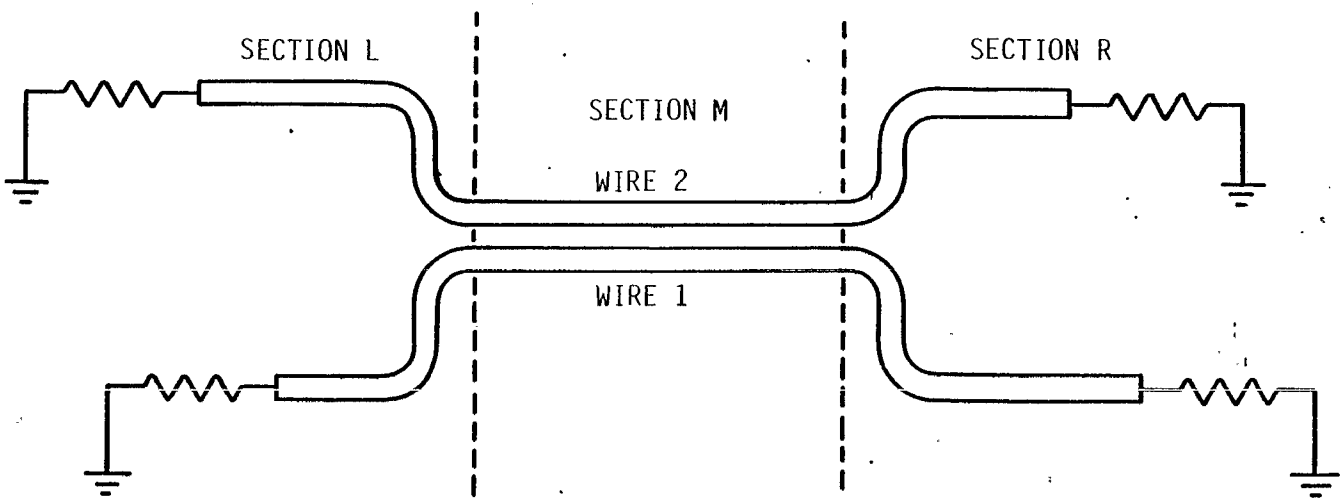

Figure 13. Two-wire plus ground MTL used to illustrate a rate-equation method of treating the energy flow of an excited MTL.

$$\bar{\bar{T}} = 2\bar{\bar{C}}_R(\bar{\bar{C}}_R + \bar{\bar{C}}_L)^{-1} \tag{55}$$

But the energy to the left of the junction is

$$W_L = 2\bar{I}_L^{+T}\,\bar{\bar{L}}_L\,\bar{I}_L^{+} \tag{56}$$

Therefore, Equation 53 is rewritten

$$\bar{I}_L^{+T}\,\bar{\bar{T}}^T\,\bar{\bar{C}}_R^{-1}\,\bar{\bar{T}}\,\bar{I}_L^{+} = F_{LR}\,\bar{I}_L^{+T}\,\bar{\bar{C}}_L^{-1}\,\bar{I}_L^{+} \tag{57}$$

For most cable configurations, as illustrated in the example in the Section III, the eigenvalues of $\bar{\bar{T}}$ will be very close to pure common, $I_c^T = (1,1)$, and differential, $I_d^T = (1,-1)$, modes. Using this assumption, the energy transmission coefficient for common modes is

$$F_{LR}^c = \bar{I}_c^T\,\bar{\bar{T}}^T\,\bar{\bar{C}}_R^{-1}\,\bar{\bar{T}}\,\bar{I}_c / \bar{I}_c^T\,\bar{\bar{C}}_L^{-1}\,\bar{I}_c \tag{58}$$

and the coefficient for differential modes is

$$F_{LR}^d = \bar{I}_d^T\,\bar{\bar{T}}^T\,\bar{\bar{C}}_R^{-1}\,\bar{\bar{T}}\,\bar{I}_d / \bar{I}_d^T\,\bar{\bar{C}}_L^{-1}\,\bar{I}_d \tag{59}$$

It is appropriate to define the matrix

$$\bar{\bar{F}}_{LR} = \begin{pmatrix} F_{LR}^c & 0 \\ 0 & F_{LR}^d \end{pmatrix} \tag{60}$$

A similar matrix $\bar{\bar{F}}_{RL}$ may be defined for the energy flow from the right section of line to the left section. $\bar{\bar{F}}$ acts on vector $\bar{W} = (W_c, W_d)$.

Rate equations for the energy flow in a transmission line will be derived for a sample case in this section. A simplified cable bundle is shown in Figure 13.

An energy S(t) is introduced into section M, entirely as a common mode. The rate equation for the energy in section M is

$$\dot{\overline{U}}_M(t) = \overline{\overline{Z}}_M \dot{\overline{W}}_M(t) = (v/2)\left[-\overline{\overline{F}}_{MR}\,\overline{W}_M(t) - \overline{\overline{F}}_{ML}\,\overline{W}_M(t) + \overline{\overline{F}}_{RM}\,\overline{W}_R(t) + \overline{\overline{F}}_{LM}\,\overline{W}_L(t)\right] + \dot{S}(t)\begin{pmatrix}1\\1\end{pmatrix} \quad (61)$$

where $\overline{\overline{Z}}_M$ is a diagonal matrix with the lengths of the two middle wires as its elements and the dot represents the time derivative. The rate equation for the energy in section L is

$$\overline{\overline{Z}}_L \dot{\overline{W}}_L(t) = (v/2)\left[\overline{\overline{Q}}\,\overline{\overline{F}}_{ML}\,\overline{W}_M(t) - \overline{\overline{F}}_{LM}\,\overline{\overline{Q}}\,\overline{W}_L(t) - \overline{\overline{F}}_{LG}\,\overline{W}_L(t)\right] \quad (62)$$

where $Q_{ij} = 1/2$ for all elements. If half the wavelength is short compared to the lengths of wire 1 and wire 2 to the left of the junction, then the expectation for the returning current will be evenly mixed between common and differential modes. Because there is no mutual capacitance in section L, the energy is the same for a common mode as for a differential mode in that section. Thus, Q puts half the energy in the common mode and half the energy in the differential mode. The energy flow through the end of each wire is a diagonal element of $\overline{\overline{F}}_{LG}$.

Similarly, the rate equation for the energy in section R is

$$\overline{\overline{Z}}_R \dot{\overline{W}}_R = (v/2)\left[\overline{\overline{Q}}\,\overline{\overline{F}}_{MR}\,\overline{W}_M - \overline{\overline{F}}_{RM}\,\overline{\overline{Q}}\,\overline{W}_M - \overline{\overline{F}}_{RG}\,\overline{W}_M\right] \quad (63)$$

The rate equations 61 through 63 may be solved for $\overline{W}_R(t)$, $\overline{W}_L(t)$, and $\overline{W}_M(t)$.

The current in the differential mode, in the left section is

$$I_d = \left[v^2 W_d / \overline{I}_d^T \overline{\overline{C}}_L^{-1} \overline{I}_d\right]^{1/2} \quad (64)$$

where $\overline{I}_d^T = (1,-1)$, and the current in the common mode is

$$I_c = \left[v^2 W_c / \overline{I}_c^T \overline{\overline{C}}_L^{-1} \overline{I}_c\right]^{1/2} \quad (65)$$

where $\overline{I}_c^T = (1,1)$.

The peak current is the sum of I_d and I_c, while the average current is the root sum square of them.